1Pb3-3

Fundamental study of 2-2 ceramic-air composite transducers for air-coupled ultrasonic measurement

空中超音波計測のための 2-2 圧電セラミック空気コンポジットの基礎研究

Hitoshi Kumagai[1†], Toshihiro Tsuji[1], Yoshikazu Ohara[1], and Tsuyoshi Mihara[1]
([1]Tohoku Univ.)
熊谷　仁志 [1†], 辻　俊宏 [1], 小原　良和 [1], 三原　毅 [1] ([1] 東北大)

1. Introduction

The improvement of a piezoelectric transducer is essential to extend the application field of nondestrictive testing with air-coupled ultrasound. 1-3 composite between piezoelectric ceramics and air (air composite) was applied to air-coupled transducer combined with acoustic coupling multilayer, leading to commercially available best transducer.[1-3] We prototyped the air composite with elctrodes of acoustically thin front plate,[4] and found that the sound source due to local deflection vibration could be useful for large amplitude transmission,[5] where the principle might be related to intense airterial ultrasound source of low frequency[6] However, the source area is limited up to 20 % of the whole area to obtain practical robustness. The purpose of this study is to develop 2-2 air composite expanding the area over 50%. We studied the effect of the front plate material on the waveform using finite element analysis (FEA).

2. FEA of air transmission

Figure 1 shows schematics of FEA model. Two-dimensional analysis was performed to reduce the calculation cost with OnScale™. A transducer is composed of a backing, a piezoelectric element and a front plate **[Fig.1 (a)]**. The materials are depolarized PZT ceramics ($t_{\mathrm{B}} = 4$ mm) for the backing, soft-type PZT ceramics of high piezoelectric constant and low Q factor ($l = 1$ mm, Fujiceramics, C9) for the piezoelectric element, pure Al or polyimide (PI) for the front plate. The piezoelectric element is 2-2 structure with PZT of an aspect ratio of 2 ($a = 0.5$ mm) and 0.9 mm-depth gap ($w = 1.0$ mm). The thickness of the front plate (t_{F}) was determined to make the deflection resonance frequency about 350 kHz. As a result, $t_{\mathrm{F}} = 0.09$ mm for Al and $t_{\mathrm{F}} = 0.5$ mm for PI.

Figure 1(b) shows air-transmission analysis model, where whole area was 34 mm x 75 mm by 0.05 mm voxel mesh and the absorption boundary was set on the boundary. The transducer with an aperture of 14 mm was excited by 30-cycles tone burst signal (400 V) at the resonance frequency. 281 received points were set at 50mm from the transducer with the same aperture as a receiver.

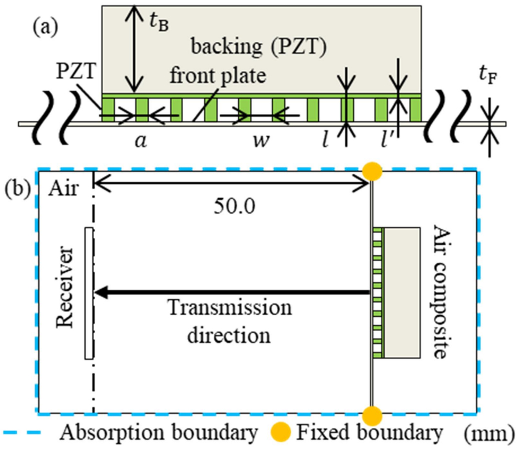

Fig. 1 Schematics of FEA model. (a) 2-2 composite transducer and (b) air-transmission analysis.

3. Result

3.1 Resonance characteristics

Figure 2 shows the impedance spectra, where f_F and f_P show the resonance frequencies of the front plate (operating frequency) and the piezoelectric element, respectively. The magnitude at f_F of PI front plate transducer (PI transducer) was lower than that of Al front plate transducer (Al transducer), with the phase closer to 0°.

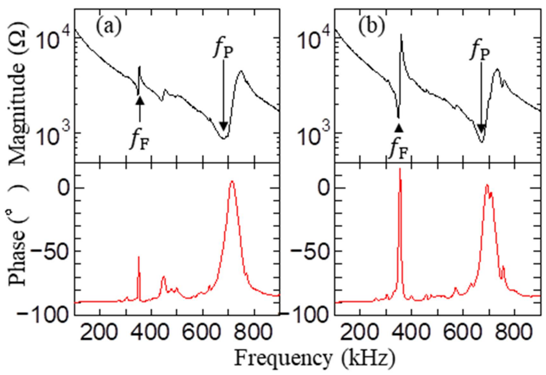

Fig. 2 Impedance spectra. (a) Al front plate transducer, (b) PI front plate transducer.

Figures 3 show the resonance modes at f_F, where color bar represents the magnitude of the x-component particle velocity qualitatively. There was large phase delay at both ends of the aperture in Al transducer, in spite of large amplitude generation **[Fig. 3(a)]**. In addition, the particle velocity was non-uniform in the backing near the piezoelectric element. However, significant phase delay was not observed in PI transducer **[Fig. 3(b)]**.

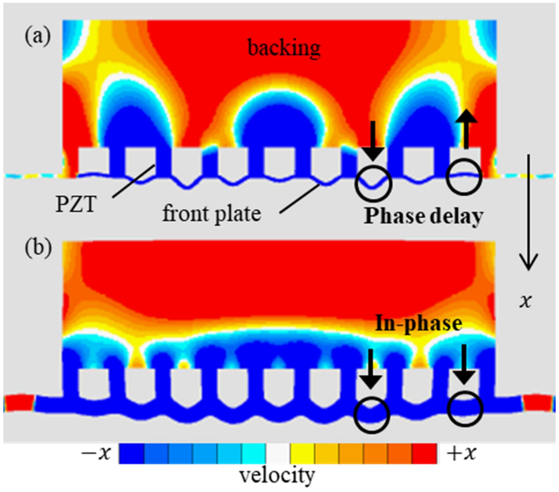

Fig. 3 Resonance modes at the f_F. (a) Al front plate, (b) PI front plate.

3.2 Particle velocity on front plate

Figure 4 shows x-component particle velocity waveforms on the front plate, where "Excitation" represents the period of the burst signal excitation. A is a result on the PZT, B and C are the results on a gap near the PZT and at the center, respectively. Each amplitude increased monotonically as the excitation progressed. The maximum amplitude at C of PI transducer was 0.67 times smaller than that of Al transducer. However, the amplitude at A in PI transducer was 4.9 times larger. Therefore, it was found that PI front plate was effective to reduce the amplitude non-uniformity.

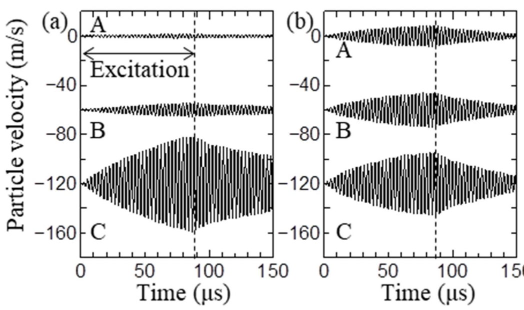

Fig. 4 Particle velocity waveforms on front plate. (a) Al front plate, (b) PI front plate.

3.3 Propagation characteristics

Figure 5 shows acoustic pressure distributions at 140μs, where thick line represents the transducer. The main robe in PI transducer was clearer than that in Al transducer, less affected by the grating robe. Moreover, the side robe in PI transducer was significantly decreased.

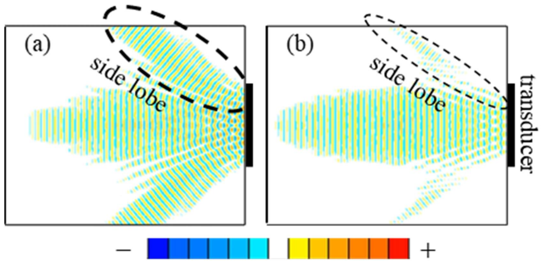

Fig. 5 Acoustic pressure distributions at 140μs from excitation. (a) Al front plate, (b) PI front plate.

Figure 6 shows x-component particle velocity waveform at 50mm. The maximum amplitude in PI transducer was 1.14 times larger than that of Al transducer. PI front plate is more effective than the Al one.

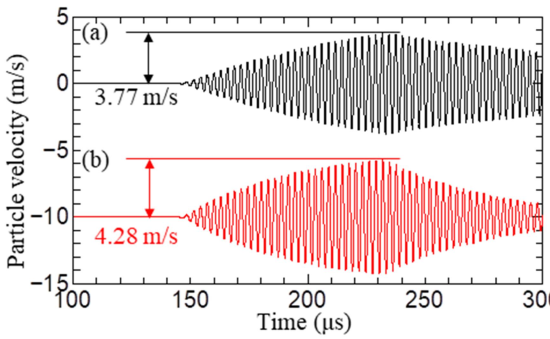

Fig. 6 Particle velocity waveforms at 50mm in air. (a) Al transducer, (b) PI transducer.

4. Conclusion

The front plate material should be chosen as improving the phase uniformity of the transmission wave front. We will verify it by prototyping and survey the material capable of expanding the gap width at 400 kHz.

References

1. M. C. Bhardwaj: US Patent 6,311,573 (2001).
2. M. C. Bhardwaj: US Patent 7,382,082 (2008).
3. M. C. Bhardwaj: Mat. Res. Innovat. **1** (1997) 188.
4. C. Oakley and P. Marsh: Proc. SPIE **1733** (1992) 274.
5. H. Ohshida, H. Kumagai, T. Tsuji, Y. Ohara, T. Mihara: Proc. Symp. Ultrason. Electron. **41** (2020) 3J3-2.
6. Y. Ito: Acoust. Sci. & Tech. vol. 36, no. 3 (2015)